Research Article Vol. 12, No. 4 / 1 April 2021 / Biomedical Optics Express 1821
Biomedical Optics EXPRESS

Static compression optical coherence elastography to measure the mechanical properties of soft contact lenses

ZACHERY QUINCE,* DAVID ALONSO-CANEIRO, SCOTT A. READ, AND MICHAEL J. COLLINS

Queensland University of Technology (QUT), Centre for Vision and Eye Research, School of Optometry and Vision Science, Kelvin Grove, Queensland, Australia
zach.quince@hdr.qut.edu.au

Abstract: In this study, a novel method was developed for estimating the elastic modulus (Young's modulus) of soft contact lens materials using static compression optical coherence elastography. Using a commercially available spectral domain optical coherence tomography instrument, an experimental setup was developed to image a soft contact lens sample before and during compression with a known applied force, from which the lens material's mechanical properties can be derived. A semi-automatic segmentation method using graph-search theory and dynamic processing was used to trace the lens boundaries and to determine key structural changes within the images. To validate the method, five soft contact lens materials with a range of known elastic moduli and water contents were tested. The proposed method was successful in estimating the Young's modulus in the five different soft contact lens materials. It was demonstrated that the method provides highly repeatable measurements, with an intraclass correlation coefficient of >95%. The Young's modulus results were compared to published manufacturer data with no significant difference for four out of the five materials ($p > 0.05$). These results demonstrate that a static compression optical coherence tomography method can reliably measure the elastic modulus of soft contact lenses. This provides a methodology that can be used to explore in vitro contact lens mechanical properties, but more importantly, may also be extended to study the mechanical characteristics of in vivo or ex vivo tissue, provided that they can be imaged using OCT.

1. Introduction

Soft contact lenses are the most commonly used contact lens modality in clinical practice, since they are generally more comfortable to wear than rigid material lenses, whilst still providing stable vision correction [1]. Almost 90% of contact lens wearers use soft contact lenses [2]. Since comfort is a key factor in successful soft contact lens wear, manufacturers need to carefully consider the lens material when designing lenses. Due to this, there is an inherent trade-off where the lens must be rigid enough to allow patient handling, insertion and removal, and should not deform on the eye during blinking, thereby maintaining visual quality, whilst also being soft enough to wrap to the surface of the eye and minimize mechanical interaction with the eyelids during blinking to maintain comfort [3,4].

Contact lens rigidity is influenced by both the thickness of the lens and the material properties [4]. The mechanical properties of a contact lens are typically defined by the elastic modulus (Young's modulus) of the material. Soft contact lenses are manufactured from a variety of polymers, of differing oxygen permeability and water content, which influences their mechanical properties. For example, newer soft contact lens materials, such as silicone hydrogels, have superior oxygen transmissibility compared to traditional hydrogel materials (e.g. HEMA-based lenses), as silicone enhances the oxygen transport through the lens. Hydrogel lenses typically

#419344 https://doi.org/10.1364/BOE.419344
Journal © 2021 Received 7 Jan 2021; revised 12 Feb 2021; accepted 23 Feb 2021; published 2 Mar 2021

Biomedical Optics EXPRESS

contain between 30 to 80% water content [4], while silicone hydrogels have water contents ranging from 24 to 74% [5]. A stiffer silicone hydrogel material such as Lotrafilcon A has a high modulus of approximately 1.4 MPa with a low water content of 24%, while a softer hydrogel material such as Etafilcon A, has a higher water content of 58% with a low modulus of 0.2 MPa.

The Young's modulus of a material or tissue is given by the relationship between its stress and strain characteristics. By characterizing this relationship, Young's modulus can be calculated by fitting a linear equation to the stress-strain data. However, this linear relationship is only valid until the material reaches a certain point (yield point) at which the deformation becomes permanent. This behavior needs to be taken into consideration when characterizing the material mechanical properties, approximating a linear relationship and extracting the Young's modulus. Typically, for contact lens materials, a linear relationship has been documented for a strain rate ranging from 0 up to 8% [4], 10% [3], 15% [6] and 40% [7].

To directly measure contact lens mechanical properties, two principles can be used: compression or tension. A tensile test is a standardized test to determine the mechanical properties of a material, in which the sample is placed between two clamps and is loaded via stretching. The method utilizes an actuator that pulls the material while the change in the length of the material is measured using a strain gauge attached to the sample. Tensile testing has been previously used to characterize contact lens mechanical properties [8]. On the other hand, a compressive test loads the sample through compression and measures the dimensions of the material before and during compression to determine the strain. If the force of the compression is measured simultaneously, the stress can also be determined. A number of studies have used the compression principle to characterize contact lens mechanical properties [9–11].

Using these two principles of compression or tension, a variety of techniques have been applied to measure contact lens material properties. A compressive nano-indentation method was utilized by Selby et al. [9] to examine the mechanical properties of soft contact lenses, while Kim et al. [4] used a custom-built MicroTensometer to measure the stretch and release characteristics of soft contact lenses at room temperature though tensile testing. Horst et al. [7] used a BioTester (CellScale Biomaterials Testing, Waterloo, Canada) to measure the elasticity of contact lens strips. This method varies from a typical tensile test as the sample is not clamped, but rather it is pulled via BioRakes (BT-305-10) inserted in each lateral side of the sample with five electro-mechanical tips that insert into the material.

In recent years, elastography techniques have become a popular method for determining the mechanical properties of samples using imaging methods. Through stimulation of the sample (movement or compression) while imaging, the variation in the images can be quantified to determine the mechanical properties of the sample. There are multiple ways that the material can be loaded in elastography, including static, transient and vibrational stimulation [12]. Each of these requires different acquisition protocols and provides different insight into the mechanical properties of the sample. Optical coherence elastography (OCE) encompasses the application of elastography principles using optical coherence tomography (OCT) as the imaging method. OCT is an imaging modality widely utilized in the field of optometry and ophthalmology [12], to capture high-resolution cross-sectional (B-scan) or volumetric scans of tissue at a micron scale [12]. By capturing sequential images of a material before and during loading, the mechanical properties can be inferred through image analysis.

OCT imaging has been widely used in a range of contact lens imaging applications, particularly to measure the thickness of contact lenses, both in vitro and in vivo. Karnowski et al. [13] used a swept source OCT to image soft and rigid contact lenses to accurately and precisely characterize central thickness, diameter and power in vitro. Hall et al. [14] investigated the influence of corneoscleral junction topography on the effective fit of soft contact lenses. A study by Martin et al. [15] investigated the changes of corneal thickness and shape caused by contact lens wear, demonstrating that repeatable corneal thickness measurements could be taken without removing

Biomedical Optics EXPRESS

the contact lens. Using OCT imaging, Kaluzny et al. [16] demonstrated in vitro changes of the geometry of soft contact lenses after a period of 7 consecutive days of lens wear. Those studies have shown that imaging and characterization of contact lenses is possible both in vivo and in vitro using OCT.

Compression OCE has been previously used in the quantification of biomaterials. Meng et al. [17] used a compression OCE method to measure homogenous silica gel phantoms, two-layer phantoms and animal tissue in three-dimensions. The method showed good agreement with the results provided by a tensile test performed on the same samples. A study by Ko et al. [18] used compression OCE to measure an engineered tissue model containing NIH-3t3 cells within a collagen matrix, using polystyrene microspheres as an optical scatterer. The method was able to measure the displacement fields of the samples under loading. Kennedy et al. [19] used a compression based OCE technique that incorporated the use of a compliant stress sensor. The experimental setup was able to determine the elasticity of a silicone phantom using a ring actuator that compressed the sample. An extension of this principle was also used to image cells and the extracellular matrix by Hepburn et al. [20]. These studies demonstrate the potential of using compression OCE to characterize biomaterial mechanical properties. However, they have generally relied on sophisticated optical setups that cannot be easily adopted by other researchers or used clinically, this study uses a commercial SD-OCT with minimal hardware modifications, to provide a tool to characterize contact lens biomechanical properties that may be easily replicated by other groups, and the potential for clinical translation in the future.

Similarly, OCE has been used to measure mechanical properties in ex vivo corneas. Ford et al. [21] used a Fourier domain OCT and clinical applanation technique to load the tissue. Kling et al. [22] used a quasi-static OCE method, that uses intraocular pressure changes to induce ex vivo corneal loading and to explore anterior and posterior stroma mechanics. However, the use of a static compression OCE method to directly measure contact lens mechanical properties has not been previously reported. By using an OCT instrument, a set of scans (both pre and during compression) can be taken to capture the changes in a volumetric section of the material, at a micron scale resolution. Thus, using a commercially available OCT instrument with limited hardware additions allows the potential characterization of the mechanical properties of contact lens materials.

The purpose of this study was to develop and validate a novel method to measure the mechanical properties of soft contact lenses, using OCE principles and static compression. By taking a volumetric scan of a contact lens with a commercial spectral domain OCT (SD-OCT) instrument before and during compression, and applying the principles of elastography, the mechanical properties of the lens were derived. To validate the method, a range of commonly used soft contact lenses materials were tested and the estimated Young's modulus was compared with those reported in the literature.

2. Methodology

This section provides a detailed overview of the methods, including the theoretical principle the method is based on, as well as the details of the hardware and imaging components of the setup. The details of the tested contact lens materials are also provided.

2.1. Theoretical principles

The static compression OCE method aims to analyze OCT images of a contact lens sample captured before and during mechanical compression by a glass plate. The Young's modulus (E, in MPa) of the material is derived as the ratio between the stress (σ, in MPa) and the strain (ε, unitless) values using (1) (assuming uniaxial compression)

$$E = \frac{\sigma}{\varepsilon} \tag{1}$$

Biomedical Optics EXPRESS

In this study, the strain can be estimated by measuring the contact lens boundaries before and during compression using the corresponding OCT images and the calculation given by (2).

$$\varepsilon = \frac{L_o - L_N}{L_o} \tag{2}$$

Where, L_O is the 'original' thickness of the contact lens before compression and L_N is the 'new' thickness of the contact lens during compression, both in µm. Finally, the stress value is estimated from the force that the contact lens is under during compression using (3).

$$\sigma = \frac{F}{A} \tag{3}$$

Where, F is the force in Newtons (N) and A is the cross-sectional area in m^2 measured by imaging the surface of the contact lens using the en face scanning laser ophthalmoscope (SLO) image to extract the radius. It should be noted that the model used for estimating the mechanical properties assumes that the strain and internal stress are uniaxial, and no friction occurs between surfaces. To satisfy these assumptions, the setup was calibrated to ensure the compression plate was parallel to the sample, and therefore the applied force would be uniaxial. Soft contact lenses can exhibit viscoelastic properties that for the purpose of this study are assumed to be negligible.

2.2. Hardware component

The method is comprised of two parts: the imaging side and the sample side. The "imaging side" of the experimental setup (Fig. 1(b)) consisted of a transparent compression plate (glass) attached to the imaging head of the Spectralis OCT instrument (Heidelberg Engineering GmbH, Germany) using a 3D printed attachment. The commercial OCT instrument uses a super luminescence diode (SLD) operating at a central wavelength of 870 nm and has an optical resolution of 7 µm (axial) and 30 µm (lateral). The axial range of the OCT is 1.9 mm (in tissue). The "sample side" of the experimental setup (Fig. 1(c)) consisted of a mount that held a Digimatic micrometer head series 164 (Mitutoyo, Aurora, IL) on the OCT instrument head rest and a force sensor.

The micrometer head, which allowed the fine adjustments (1 µm movement resolution) needed for micro-levels of compression, was used to displace the sample (contact lens) towards the compression plate. The force sensor is located between the micrometer head and the sample. As the force sensor had a highly reflective metallic surface, a 3D printed sample mount was used as an interface to separate the contact lens and force sensor to remove the optical reflections from the metallic surface. Both the flat glass compression plate and sample mount were made out of a rigid material that would not deform under the compression levels used in this experiment to deform the contact lens. The force sensor (FSAGPNXX1.5LCAC5 – Honeywell, Charlotte, NC) is a fully calibrated piezoresistive-based force sensor offering a ratio-metric analog output for determining force over a specified full-scale force span and temperature range (temperature compensated). To calculate the force (F) throughout the experiment (4) was used, which converts the sensor's output voltage into force from the transfer function provided by the manufacturer.

$$F = \frac{F_R(V_o - 0.2V_s)}{0.6V_s} \tag{4}$$

The force range (F_R) was the range that the sensor could read, which for the selected sensor was a constant value of 6.67 N. The output voltage V_O was the voltage that was read from the output pin on the sensor and V_S was the supply voltage, which was set at 5 V throughout the experiment. Both voltages (V_O and V_S) were recorded for each compression using two digital multimeters, with the output voltage accuracy of ± 0.5% and the supply voltage accuracy of ± 0.8%. Since this sensor was a major component of the experiment, used to extract the force value for the stress

Biomedical Optics EXPRESS

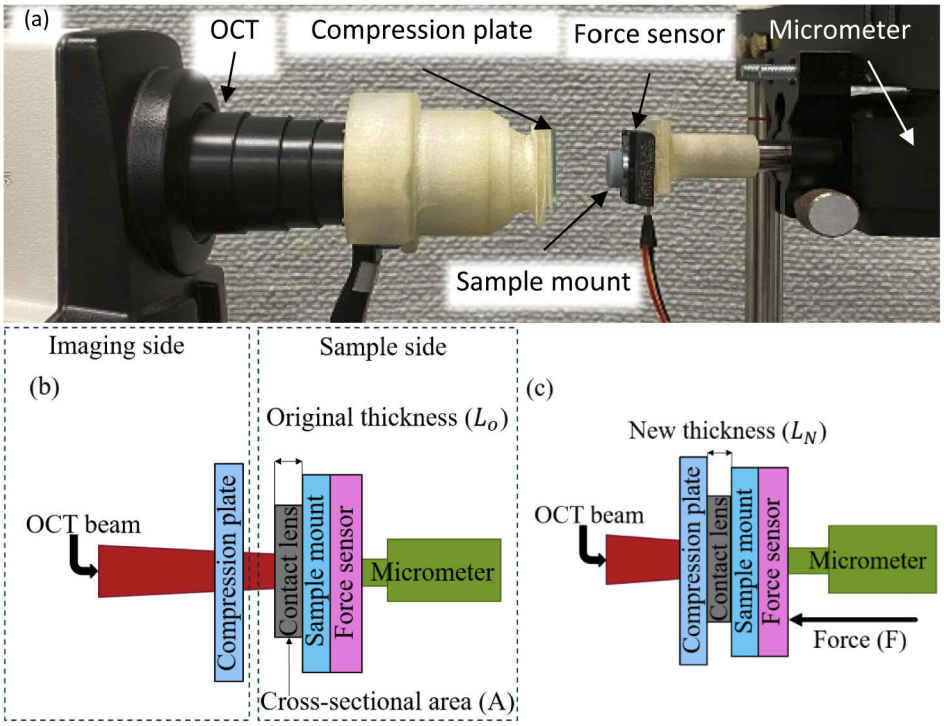

Fig. 1. Schematic diagram of the static compression OCE methodology, showing the experimental setup (a), a diagram of the pre compression setup (b) where, A is the cross-sectional area, LO is the original contact lens thickness and a diagram of the compression image setup (c) with the micrometer compressing the contact lens into the compression plate, where F is the applied force, and LN is the new thickness.

component, a preliminary validation of the sensor was performed prior to using it in the setup. The sensor unit was subjected to increasing forces by a spring gauge. To ensure the different interfaces would not affect the final measurements, the sensor was initially tested directly on the spring gauge, then a glass plate was added to the spring gauge and finally a contact lens was introduced between the sensor unit and the compression plate. Five measurements were taken and averaged over a range of 0–3 N in 0.5 N steps, which was within the range of interest for the experiment and the sensor's technical specifications. The results showed a good level of agreement with the expected values, with an average (mean ± standard deviation) difference of 0.105 ± 0.083 N.

2.3. *Imaging protocol*

Using the SD-OCT instrument, the contact lenses were imaged before and during compression in order to determine their mechanical properties as shown by Fig. 2. All lenses were cut to produce a circular region of 3 mm (diameter) centered on the apex of the contact lens and this cut-out region was used as the sample to be tested. The contact lenses were imaged using a volumetric scanning protocol (approximately 8.22 mm lateral and 2.78 mm axial) using the OCT instrument's anterior segment lens attachment. The volumetric scan comprised a total of eleven B-scans (278 µm separation between B-scans) and each B-scan contained 768 A-scans. The OCT images have a transversal and axial resolution of 10.8 µm x 3.87 µm per pixel respectively. This scanning area covers the entire contact lens compression area. The instrument captures an en face image using a SLO at the same time as the volumetric OCT images. The SLO image has a

Biomedical Optics EXPRESS

uniform pixel resolution of 10.8 µm. Capturing a volumetric scan before and during compression allowed for a strain map to be calculated by (2). The strain map shows the contact lens strain (the ratio of total compression to the initial thickness) across all B-scans as a two-dimensional image. Thus, the lenses were imaged before compression to extract the original (uncompressed) thickness of the contact lens. After which, the lens was compressed by the compression plate and an additional OCT volumetric measurement under compression was captured. To ensure the measurement was taken within the linear stress-strain region, the lens was compressed to around the 10% strain region, using the voltage of the sensor as a surrogate of the force during the experiment.

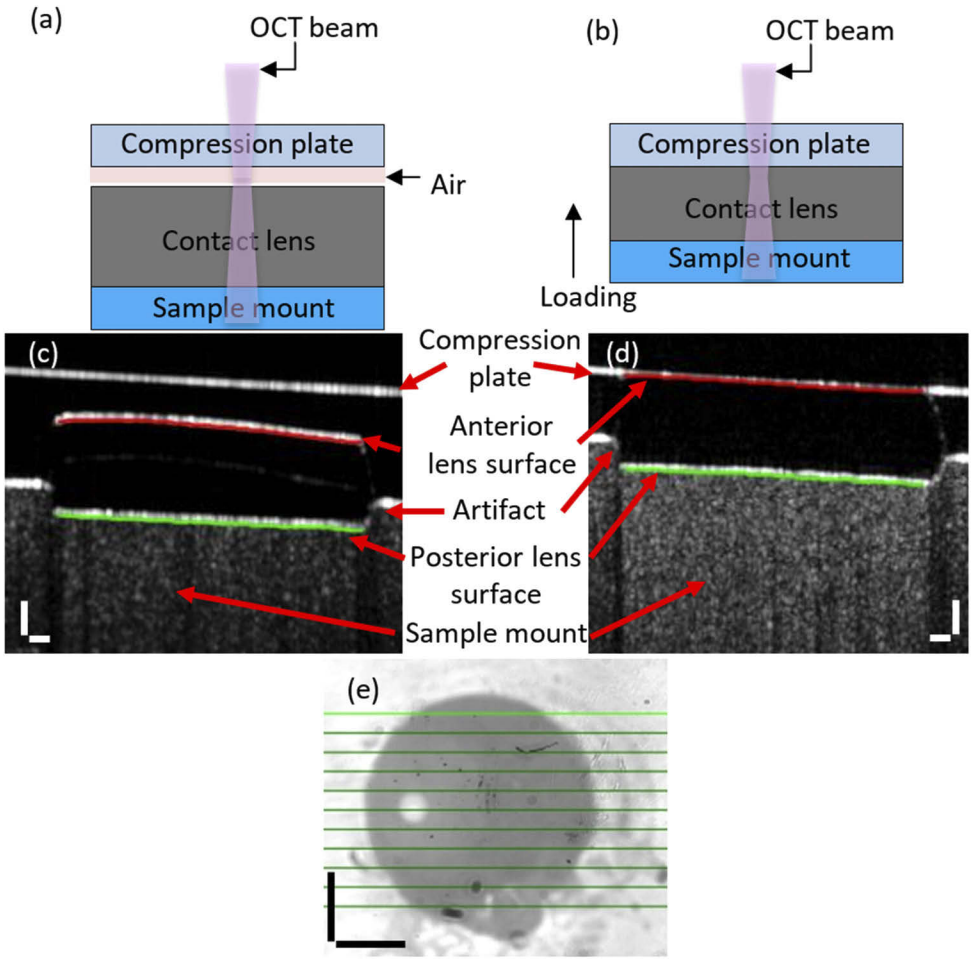

Fig. 2. (a), (b) Diagram of the capturing method for contact lenses imaged with SD-OCT, together with the corresponding OCT intensity images pre compression (c) and during compression (d) (scale – 100 µm axial, 200 µm lateral). The red and green lines correspond to the anterior and posterior surfaces of the contact lens, respectively. The artifact refers to the discontinuity in the profile close to the contact lens boundary and is due to the difference in refractive index between the contact lens and air gap past the lens. e) SLO image of the contact lens during compression with 11 B-scan lines overlaid (scale – 1 mm horizontal and vertical).

Biomedical Optics EXPRESS

2.4. Image analysis

To accurately determine the Young's modulus of the contact lenses, three key variables were calculated for each individual measurement: the contact lens surface area being compressed, the pre compression thickness and the thickness during compression. In order to determine the area for each individual lens, the SLO en face image was analyzed. A Matlab (MathWorks, Natick, MA, USA) algorithm was developed to automatically detect the contact lens outline using a circle Hough transform that allowed the calculation of the area of the contact lens sample (area of the circle) within the image. Across the entire experiment, the average (mean ± standard deviation) en face radius of compression was recorded as 1.53 ± 0.034 mm.

To calculate the strain, the change in the contact lens thickness is determined. To achieve this, the boundaries (front and back surface of the lens) of the lens were segmented to extract the thickness. A semi-automatic segmentation code, based on a previous method for OCT image segmentation [23,24] was adapted for this image analysis. The code uses graph-search theory and dynamic programming to find the layer boundaries. Each pixel is treated as a graph node, where connecting nodes are edges, which can be weighted to create a path for the segmentation to occur. To define the boundary of both the front and back surface of the contact lens, the posterior edge of these boundaries was extracted by the segmentation method.

All images and their corresponding segmented boundaries were reviewed by an observer to verify the integrity of the segmentation result, and in the case of segmentation errors, manual segmentation correction was applied. The manual segmentation code used a second order polynomial with five selected points for the anterior surface, while for the posterior surface of the lens, which is in contact and conforms to the shape of the flat sample mount, it was fit with a linear fit, also using five selected points. To ensure this manual correction process would not affect the analysis, a comparison of the segmentation methods was undertaken with each of the materials tested. For each material a set of pre and during compression volumes scan that had no segmentation errors (at least nine B-scans per volumetric scan), were manually corrected by marking all the B-scans associated with the volumetric measure. The thickness of the segmented contact lenses was compared, and the mean difference calculated. The results showed that there was an average (mean ± standard deviation) difference of 0.504 ± 0.257 pixels between fully automated and fully manual segmentation, demonstrating good agreement and no significant difference between the two methods. The OCT images showed an artifact in both sets of images (Fig. 2(c) & 2(d)), due to the difference in refractive indices of air and the contact lens material. This artefact is outside the area of measurement and will not affect the results. During compression there may be slight changes to the refractive index of the materials [25]. As the strain is low (typically 10%) it is assumed that the changes are small. Once the images were segmented, thickness profiles of the pre and during compression images could be obtained (Fig. 3(a) and Fig. 3(b)). Each of the analyzed B-scans were used to generate a thickness map of the contact lens, which were analyzed to extract the strain map (Fig. 3(c)) using (2). Using the information from the force sensor and the area, the stress was then calculated using (2) and finally, using (1), a Young's modulus map (Fig. 3(d)) was estimated. The differences recorded in the Young's modulus (Fig. 3(d)) between the outer edges and the center is due to the non-uniformity of the contact lens thickness.

To determine a singular Young's modulus value, which was later used to compare with the known manufacturer's data, a point in the Young's modulus map must be selected. This point corresponded to the thickest part of the contact lens in the pre compression images as this would represent the maximum change in thickness (i.e. maximum strain) during the compression. This particular single point was chosen, as recordings from the force sensor were representative of the maximum strain of the contact lens, which in our experiment occurred at the maximum thickness in the pre compression OCT images.

Biomedical Optics EXPRESS

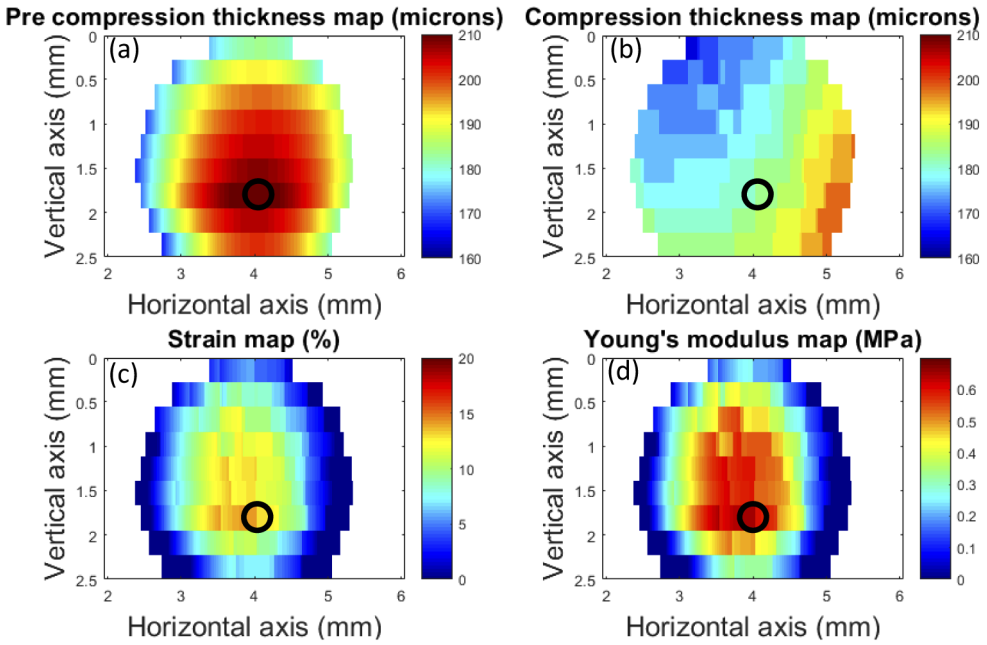

Fig. 3. Example of a recording from a representative contact lens (Omafilcon A material) showing the contact lens thickness map for the (a) pre compression and (b) during compression, together with the associated strain (c) and the Young's modulus (d) maps of the contact lens. The selection point (point of maximum strain), which is used for reporting the mechanical properties of the material, is denoted by the hollow black circle.

Throughout the experiment there were a number of factors that had to be verified to allow for a valid measurement. As the contact lens is concave in shape, it was crucial that it was placed with the back of the lens contacting the sample mount. This had to be visually inspected during the initial pre compression scan. Similarly, the lens needed to be in full contact with the surface of the force sensor to accurately determine the thickness of the lens. Lastly, to limit the reflections in the image and to remove any residual increase in the recorded thickness, any fluid on the surface of the lens had to be removed just prior to imaging, by blotting the lens.

2.5. Contact lens materials

A total of five different commercially available contact lens materials were tested: each having a different Young's modulus and water contents. Table 1 provides a summary of the main contact lens materials used. The contact lens material was cut into a circle with an approximate dimeter of 1.5 mm from the center of the lens. All the tested lenses had the same back vertex power of +6.00 Diopters. In order to assess the repeatability of the method, three lenses of each material were tested, and all lenses were imaged four times each.

There are a range of factors that can influence the mechanical properties of contact lenses [3], [26]. Soft contact lenses contain water, thus requiring consistent hydration, to minimize variations in the mechanical properties [27]. To avoid changes in material properties due to dehydration, between measurements, the lenses were immersed in a sterile saline solution (sodium chloride and potassium phosphate monobasic) for a period of at least two minutes before the lens was imaged again. The temperature of the lens has also been shown to be a key factor affecting mechanical properties [26]. The experiment was conducted in the same room and the temperature and humidity of the room were controlled. The average (mean ± standard deviation)

Biomedical Optics EXPRESS

Table 1. Selection of Contact Lens Materials Used[a]

Material	Water content	Base curve (mm)	Diameter (mm)	Thickness (μm)
Etafilcon A	58%	14.2	8.5	157
Omafilcon A	62%	14.2	8.7	216
Senofilcon A	38%	14.0	8.4	148
Lotrafilcon B	33%	13.8	8.4	162
Lotrafilcon A	24%	14.2	8.6	147

[a]Water content, base curve and diameter were extracted from manufacturer specifications. Central thickness measurements taken from OCT imaging (pre compression scans) using a +6.00 D lens and adjusting for lens refractive index.

temperature in the measurement room during testing of the lenses was 23 ± 1 °C, and the average humidity was 53 ± 5%.

2.6. Statistical analysis

To quantify the repeatability of the proposed method, a Bland-Altman analysis was performed. The 'within lens' standard deviation (S_w) was calculated from the repeated measures of Young's modulus collected on each of the lens materials. The S_w is found from taking the square root of the residual mean square error from a one-way analysis of variance (ANOVA) [28]. The repeatability coefficient (COR) was then determined based on the S_w to further quantify the repeatability of the proposed technique. This coefficient identifies the range over which 95% of repeated measurements are expected to lie. To allow comparisons between the contact lens materials, the coefficient of variation (CV) was calculated, which is the standard deviation normalized to the mean of the results. The intraclass correlation coefficient (ICC) was evaluated for the method to give further insight into the overall repeatability of the method [29]. The Young's modulus values derived in this study were compared to the previously published values for the same materials, with a one sample t-test undertaken between the current study and the manufactures specifications reported in [4], including Bonferroni adjustments to the p-values to account for multiple comparisons.

3. Results and discussion

To understand the consistency of the measurements, an initial evaluation of the repeatability of the technique is reported. The ICC was > 95% showing that the method has excellent repeatability. Table 2 summarizes the key repeatability metrics for each of the lens materials including S_w, COR and CV.

Table 2. Repeatability Analysis[a]

Material	S_w (MPa)	COR (MPa)	CV (%)
Etafilcon A	0.022	0.0599	13.75
Omafilcon A	0.052	0.1440	15.37
Senofilcon A	0.088	0.2427	13.08
Lotrafilcon B	0.1367	0.3788	12.11
Lotrafilcon A	0.1093	0.3028	6.28

[a]Sw = within lens standard deviation, COR = the repeatability coefficient, and CV = the coefficient of variation.

From the values shown in Table 2, the method presented in this study shows good repeatability for all lenses. Comparing the CV, all materials had approximately the same variation with the

Biomedical Optics EXPRESS

exception of Lotrafilcon A which showed a smaller CV. This shows that the method is repeatable across a range of mechanical and physical properties. As Lotrafilcon A has the lowest water content, this may have resulted in a lower degree of variation. Comparing to the literature, Kim et al. [4] reported a COR of < 0.1 MPa for Lotrafilcon A using a MicroTensometer technique, which is smaller than found in the current study. Using a temperature controlled tensiometer instrument, Young et al. [30] reported the COR for a range of contact lenses, a low modulus lens Galyfilcon (similar to Etafilcon A) showed a COR of 0.04 MPa and a high modulus lens (Lotrafilcon B) 0.3 MPa, which are comparable values to those reported in the current study. It should be noted that previous studies have all used different numbers of lenses and trials per lens to calculate the repeatability metrics, which may have influenced the comparisons.

Table 3 shows the Young's modulus of the five contact lens materials tested, the mean values for each of the three tested lenses per material is provided (four repetitions for each lens) as well as the average of all the lenses.

Table 3. Young's Modulus of Five Contact Lens Materials Tested (MPa)[a]

Material	Lens 1	Lens 2	Lens 3	Mean
Etafilcon A	0.163 ± 0.027	0.153 ± 0.010	0.155 ± 0.015	0.157 ± 0.022
Omafilcon A	0.304 ± 0.043	0.347 ± 0.049	0.364 ± 0.043	0.338 ± 0.052
Senofilcon A	0.706 ± 0.082	0.613 ± 0.097	0.690 ± 0.036	0.670 ± 0.088
Lotrafilcon B	1.017 ± 0.068	1.146 ± 0.171	1.225 ± 0.009	1.130 ± 0.137
Lotrafilcon A	1.874 ± 0.045	1.649 ± 0.152	1.697 ± 0.041	1.740 ± 0.109

[a]The estimate for each lens is the average of four repeated measurement trials with the mean ± standard deviation shown. The standard deviation shown for the mean is the 'within lens' metric derived from the ANOVA.

Figure 4 shows the results from the current study compared to those reported in the literature. Across all the tested materials, Senofilcon A was the closest to the reported value with a difference of 0.03 MPa between the current study and manufacturer's specification. A study by Kim et al. [4] recorded a value of 1.4 MPa for Lotrafilcon A while Young et al. [26] recorded a higher value of 2.17 MPa, which shows variability in measurements across the methods presented to date. For the Lotrafilcon A material in the current study, a measured value of 1.74 MPa was found, 0.34 MPa above [4] but 0.43 MPa lower than [26].

Overall, the results provided by the current study were comparable to the previously published literature, with the exception of Etafilcon A that was lower than previous reports. The t-test examining the difference between the current study results and the manufacturers reported values showed all materials except for Etafilcon A were not statistically significantly different ($p > 0.05$). Despite the agreement between the proposed method and the nominal values, there is a good deal of variance between the reported values. The variance across methods may be due to the different testing procedures and protocols used for each experiment.

Soft contact lenses can exhibit non-linear viscoelastic properties. For the purpose of this experiment, this behavior is assumed to be negligible for (1) and (3) to be valid, however, it is possible that the non-linearity may have impacted the results of this study. It is worth noting that the CV was better (i.e. less variable) for the lens with the lowest water content. Opdahl et al. [31] demonstrated that bulk water content changes the loading and unloading characteristics of poly(hydroxyethyl) methacrylate contact lenses. Thus, the lens water content could also be affecting the Young's modulus results, as water does not behave in the same way as the contact lens material. The effect of this viscoelastic behavior on the measurements may need to be further explored in the future.

The presented static compression OCE method provides repeatable measurements, which are also comparable to previously published results and the manufacturer's nominal values. However,

Biomedical Optics EXPRESS

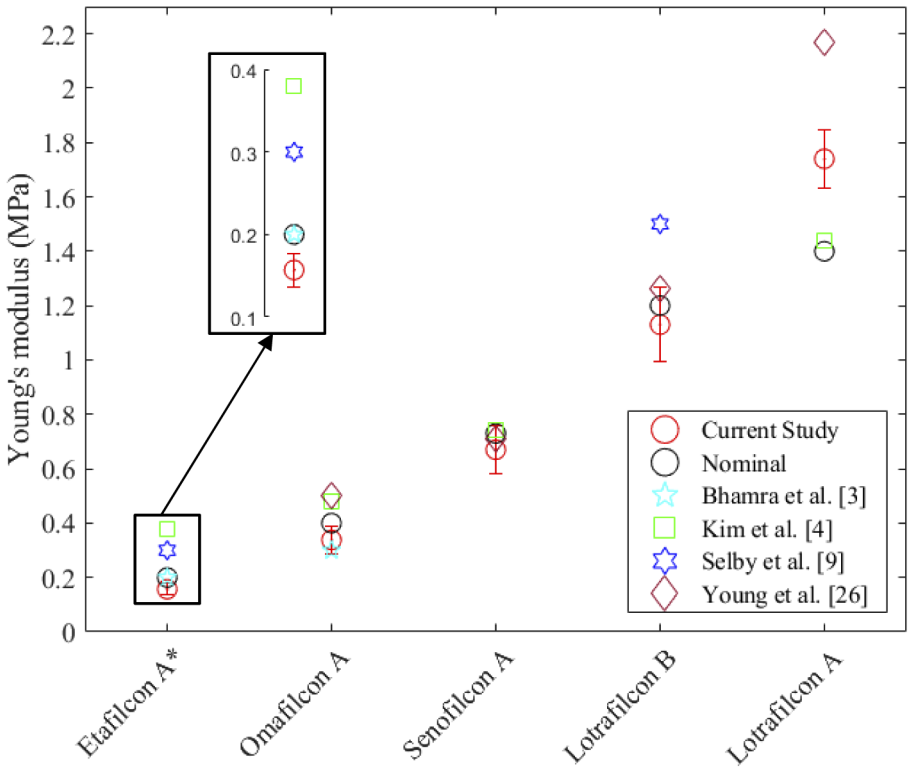

Fig. 4. Average Young's modulus of the five contact lens materials measured during this study (red circle) with error bar representing ± one standard deviation. The measured results are compared with a range of previously published values. The nominal value represents the manufacturer data for Young's modulus of each lens. The insert represents a zoomed section of the graph for the Etafilcon A material to better visualize the values.

there are several aspects of the methodology that can be improved in the future. A one-pixel difference in the OCT image can account for a strain change of up to 2%. The axial resolution of the OCT imaging therefore limits the accuracy of the method and the current segmentation code only allows for the pixels in the image to be treated as a finite scale. A graph-based framework for sub-pixel image segmentation could be adapted in the future with the proposed method to potentially improve the resolution [32]. The method also has a number of underlying assumptions including: the contact lens undergoes a uniform stress, the force is considered to be uniaxial, there is no surface friction, and contact lens viscoelastic behavior and refractive index change under compression are considered negligible. Although overall the results do seem to have a good agreement with previously published values, some of the deviation and measurement repeatability may be associated with the violation of some of the above assumptions, which should be further examined in the future.

Additionally, as the current experiment involves removing the material from its solution during the compression phase, the lens could partially dehydrate during measurements, which can result in changes in the material mechanical properties. Given that a number of the previously proposed methods used full contact lens immersion, this could also be a potential source of variability in our technique. Finally, the accuracy of the force sensor, which was used in this experiment to characterize the stress, was ± 5% of the output voltage. This leads to a variation in the recorded force of up to 0.185 N in the stiffer lens material (Lotrafilcon A lens), which would represent

Biomedical Optics EXPRESS

an approximate force variation of ± 0.231 MPa. For the soft lens material (Etafilcon A lens), there could be a difference in force of ± 0.1221 N leading to an approximate variation in Young's modulus of ± 0.094 MPa. Force sensors in the range needed for this particular application are difficult to source, but improvement in this hardware component of the setup could also result in a significant improvement in the performance of the technique.

4. Conclusions

A novel method using static compression OCE for estimating Young's modulus of soft contact lenses was presented. Five different soft contact lens materials, which encompass a wide range of mechanical properties, were tested to validate the proposed technique. Overall, the measured values were comparable to those reported in the literature using different measurement methods, demonstrating the accuracy of the proposed static compression OCE method. While this study was concerned with soft contact lens materials, future studies will focus on the extension and application of the method to other materials, including ex vivo and in vivo ocular tissues.

Disclosures. The authors declare no conflicts of interest

Data availability. Data underlying the results presented in this paper are not publicly available at this time but may be obtained from the authors upon reasonable request.

References

1. M. Chyasnavichyus, S. L. Young, and V. V. Tsukruk, "Mapping micromechanical properties of soft polymer contact lenses," Polymer **55**(23), 6091–6101 (2014).
2. B. Caffery, M. Dogru, L. W. Jones, J. J. Nichols, E. Papas, A. Pucker, H. Pult, and M. D. P. Wilcox, "Contact lens comfort," Optom Vis Sci **93**(8), 790–792 (2016).
3. T. S. Bhamra and B. J. Tighe, "Mechanical properties of contact lenses: The contribution of measurement techniques and clinical feedback to 50 years of materials development," Contact Lens and Anterior Eye **40**(2), 70–81 (2017).
4. E. Kim, M. Saha, and K. Ehrmann, "Mechanical properties of contact lens materials," Eye & Contact Lens **44**(2), S148–S156 (2018).
5. B. J. Tighe, "A decade of silicone hydrogel development: surface properties, mechanical properties, and ocular compatibility," Eye & Contact Lens **39**(1), 4–12 (2013).
6. A. Abass, S. Stuart, B. T. Lopes, D. Zhou, B. Geraghty, R. Wu, S. Jones, I. Flux, R. Stortelder, A. Snepvangers, R. Leca, and A. Elsheikh, "Simulated optical performance of soft contact lenses on the eye," PLoS ONE **14**(5), e0216484 (2019).
7. C. R. Horst, B. Brodland, L. W. Jones, and G. W. Brodland, "Measuring the modulus of silicone hydrogel contact lenses," Optom Vis Sci **89**(10), 1468–1476 (2012).
8. I. Tranoudis and N. Efron, "Tensile properties of soft contact lens materials," Contact Lens and Anterior Eye **27**(4), 177–191 (2004).
9. A. Selby, C. Maldonado-Codina, and B. Derby, "Influence of specimen thickness on the nanoindentation of hydrogels: measuring the mechanical properties of soft contact lenses," J. Mech. Behav. Biomed. Mater. **35**, 144–156 (2014).
10. M. Robitaille, J. Shi, S. McBride, and K.-T. Wan, "Mechanical performance of hydrogel contact lenses with a range of power under parallel plate compression and central load," J. Mech. Behav. Biomed. Mater. **22**, 59–64 (2013).
11. C. Li, M. Ahearne, and K.-K. Liu, "Micromechanical characterization of hydrogel-based contact lens," Int. J. Mod. Phys. B **24**(01n02), 117–127 (2010).
12. M. A. Kirby, I. Pelivanov, S. Song, Ł. Ambrozinski, S. J. Yoon, L. Gao, D. Li, T. T. Shen, R. K. Wang, and M. O'Donnell, "Optical coherence elastography in ophthalmology," J. Biomed. Opt. **22**(12), 1 (2017).
13. K. Karnowski, I. Grulkowski, N. Mohan, I. Cox, and M. Wojtkowski, "Quantitative optical inspection of contact lenses immersed in wet cell using swept source OCT," Opt. Lett. **39**(16), 4727–4730 (2014).
14. L. A. Hall, G. Young, J. S. Wolffsohn, and C. Riley, "The influence of corneoscleral topography on soft contact lens fit," Invest. Ophthalmol. Visual Sci. **52**(9), 6801–6806 (2011).
15. R. Martin, M. Izquierdo, and A. Saber, "Investigation of posterior corneal curvature in CL-induced corneal swelling," Contact Lens and Anterior Eye **32**(6), 288–293 (2009).
16. B. J. Kaluzny, J. Stachura, P. Mlyniuk, A. Jimenez-Villar, M. Wietlicka-Piszcz, and I. Grulkowski, "Change in the geometry of positive-and negative-powered soft contact lenses during wear," PLoS ONE **15**(11), e0242095 (2020).
17. F. Meng, X. Zhang, J. Wang, C. Li, J. Chen, and C. Sun, "3D strain and elasticity measurement of layered biomaterials by optical coherence elastography based on digital volume correlation and virtual fields method," Appl. Sci. **9**(7), 1349 (2019).
18. H.-J. Ko, W. Tan, R. Stack, and S. A. Boppart, "Optical coherence elastography of engineered and developing tissue," Tissue Eng. **12**(1), 63–73 (2006).

Biomedical Optics EXPRESS

19. K. M. Kennedy, L. Chin, R. A. McLaughlin, B. Latham, C. M. Saunders, D. D. Sampson, and B. F. Kennedy, "Quantitative micro-elastography: imaging of tissue elasticity using compression optical coherence elastography," Sci. Rep. **5**(1), 15538 (2015).
20. M. S. Hepburn, P. Wijesinghe, L. G. Major, J. Li, A. Mowla, C. Astell, H. W. Park, Y. Hwang, Y. S. Choi, and B. F. Kennedy, "Three-dimensional imaging of cell and extracellular matrix elasticity using quantitative micro-elastography," Biomed. Opt. Express **11**(2), 867–884 (2020).
21. M. R. Ford, W. J. Dupps, A. M. Rollins, A. S. Roy, and Z. Hu, "Method for optical coherence elastography of the cornea," J. Biomed. Opt. **16**(1), 016005 (2011).
22. S. Kling, E. A. Torres-Netto, B. Spiru, W. Sekundo, and F. Hafezi, "Quasi-static optical coherence elastography to characterize human corneal biomechanical properties," Invest. Ophthalmol. Visual Sci. **61**(6), 29 (2020).
23. S. J. Chiu, X. T. Li, P. Nicholas, C. A. Toth, J. A. Izatt, and S. Farsiu, "Automatic segmentation of seven retinal layers in SDOCT images congruent with expert manual segmentation," Opt. Express **18**(18), 19413–19428 (2010).
24. D. Alonso-Caneiro, S. A. Read, and M. J. Collins, "Automatic segmentation of choroidal thickness in optical coherence tomography," Biomed. Opt. Express **4**(12), 2795–2812 (2013).
25. H. Zeng, J. Wang, Q. Ye, Z. Deng, J. Mei, W. Zhou, C. Zhang, and J. Tian, "Study on the refractive index matching effect of ultrasound on optical clearing of bio-tissues based on the derivative total reflection method," Biomed. Opt. Express **5**(10), 3482–3493 (2014).
26. G. Young, R. Garofalo, S. Peters, and O. Harmer, "The effect of temperature on soft contact lens modulus and diameter," Eye & Contact Lens **37**(6), 337–341 (2011).
27. A. Barnes, P. H. Corkhill, and B. Tighe, "Synthetic hydrogels: 3. Hydroxyalkyl acrylate and methacrylate copolymers: surface and mechanical properties," Polymer **29**(12), 2191–2202 (1988).
28. J. M. Bland and D. G. Altman, "Measuring agreement in method comparison studies," Stat Methods Med Res **8**(2), 135–160 (1999).
29. M. P. W. Leslie and G. Portney, *Foundations of Clinical Research: Applications to Practice*, 3rd Edition (Prentice Hall, 2008).
30. G. Young, R. Garofalo, O. Harmer, and S. Peters, "The effect of soft contact lens care products on lens modulus," Contact Lens & Anterior Eye **33**(5), 210–214 (2010).
31. A. Opdahl, S. H. Kim, T. S. Koffas, C. Marmo, and G. A. Somorjai, "Surface mechanical properties of pHEMA contact lenses: viscoelastic and adhesive property changes on exposure to controlled humidity," J. Biomed. Mater. Res. **67A**(1), 350–356 (2003).
32. F. Malmberg, J. Lindblad, N. Sladoje, and I. Nyström, "A graph-based framework for sub-pixel image segmentation," Theoretical Computer Science **412**(15), 1338–1349 (2011).